

3-D seismic images of an extensive igneous sill in the lower crust

T. Wrona^{1,2*}, C. Magee^{3,4}, H. Fossen⁵, R.L. Gawthorpe¹, R.E. Bell³, C.A.-L. Jackson³, and J.I. Faleide⁶

¹Department of Earth Science, University of Bergen, Allégaten 41, N-5007 Bergen, Norway

²Norwegian Academy of Science & Letters (VISTA), Drammensveien 78, 0271 Oslo, Norway

³Basins Research Group, Department of Earth Science and Engineering, Imperial College, Prince Consort Road, London SW7 2BP, UK

⁴School of Earth and Environment, University of Leeds, Leeds LS2 9JT, UK

⁵Museum of Natural History, University of Bergen, Allégaten 41, N-5007 Bergen, Norway

⁶Department of Geosciences, University of Oslo, P.O. Box 1047 Blindern, N-0316 Oslo, Norway

ABSTRACT

When continents rift, magmatism can produce large volumes of melt that migrate upwards from deep below the Earth's surface. To understand how magmatism impacts rifting, it is critical to understand how much melt is generated and how it transits the crust. Estimating melt volumes and pathways is difficult, however, particularly in the lower crust where the resolution of geophysical techniques is limited. New broadband seismic reflection data allow us to image the three-dimensional (3-D) geometry of magma crystallized in the lower crust (17.5–22 km depth) of the northern North Sea, in an area previously considered a magma-poor rift. The subhorizontal igneous sill is ~97 km long (north-south), ~62 km wide (east-west), and 180 ± 40 m thick. We estimate that 472 ± 161 km³ of magma was emplaced within this intrusion, suggesting that the northern North Sea contains a higher volume of igneous intrusions than previously thought. The significant areal extent of the intrusion (~2700 km²), as well as the presence of intrusive steps, indicate that sills can facilitate widespread lateral magma transport in the lower crust.

INTRODUCTION

The style of continental rifting critically depends on the strength of the lower crust (e.g., Huisman and Beaumont, 2011), which may be changed by magmatic processes including melting, magma migration, and crystallization. To study the effects of magmatism on rifting, we need to understand the distribution and volume of magma emplaced in the crust in three dimensions (e.g., White et al., 2008). While the current paradigm for magma plumbing-system structure broadly advocates that vertically stacked sills accumulate and store melt within the lower crust (e.g., Annen et al., 2005, 2015; Cashman et al., 2017; Edmonds et al., 2019), the lateral extent of these intrusion networks remains poorly understood. Three-dimensional (3-D) seismic reflection data showing acoustic images of the subsurface have revolutionized our understanding of magma plumbing systems in the upper crust (e.g., Trude et al., 2003; Planke et al., 2005). In contrast, in the lower crust, seismic studies have long been limited by data coverage and resolution, providing an incomplete picture of the geometry and distribution of lower-crustal intrusions (e.g., Cartwright and Hansen, 2006; Abdelmalak et al., 2017).

Using one of the largest 3-D seismic reflection surveys ever acquired (courtesy of CGG Worldwide, <https://www.cgg.com>), covering 35,410 km² of the northern North Sea rift and imaging down to depths of 22 km (see Texts DR1 and DR2 in the GSA Data Repository¹), we are able to

analyze lower-crustal structures at a resolution of a few tens of meters over thousands of square kilometers. This analysis allows us to critically examine and develop hypotheses for the origin of a lower-crustal reflection (LCR) that has previously been identified in sparse two-dimensional (2-D) seismic profiles (Christiansson et al., 2000; Fichler et al., 2011) but that we here are able to map in 3-D. Combining a series of detailed seismic (e.g., amplitude, polarity, continuity) and geometric observations (e.g., lobes, saucers, intrusive steps), we conclude that the LCR originates from an extensive igneous sill (~2700 km²), which previously stored significant volumes of magma (472 ± 161 km³) deep in the lower crust (17.5–22 km).

GEOLOGICAL SETTING

The study area is located in the northern North Sea (Fig. 1), where continental crust consists of 10–30-km-thick crystalline basement overlain by as much as 12 km of sedimentary strata deposited during, after, and possibly even before periods of late Permian–Early Triassic and Middle Jurassic–Early Cretaceous rifting (e.g., Bell et al., 2014; Maystrenko et al., 2017). The crystalline basement formed by terrane accretion during the Sveconorwegian (1140–900 Ma) and Caledonian (460–400 Ma) orogenies (Bingen et al., 2008). During the Caledonian orogeny, subduction of continental crust subjected some of these basement rocks to high- and ultrahigh-pressure metamorphic conditions sufficient for partial eclogitization (Austrheim, 1987). A LCR identified in older 2-D seismic reflection data imaging our study area is characterized by a high-amplitude and positive polarity, and has previously been suggested to mark the top of a kilometer-thick volume of eclogitized rocks (Christiansson et al., 2000). In contrast, based on 2-D gravity and magnetic modeling, Fichler et al. (2011) inferred that the LCR defines the boundary between overlying continental crust and an underlying, high-magnetic-susceptibility, serpentinized mantle wedge. Testing these existing hypotheses for the origin of the LCR in the context of the geodynamic evolution of the northern North Sea using 3-D seismic reflection data is the focus of this study.

OBSERVATIONS

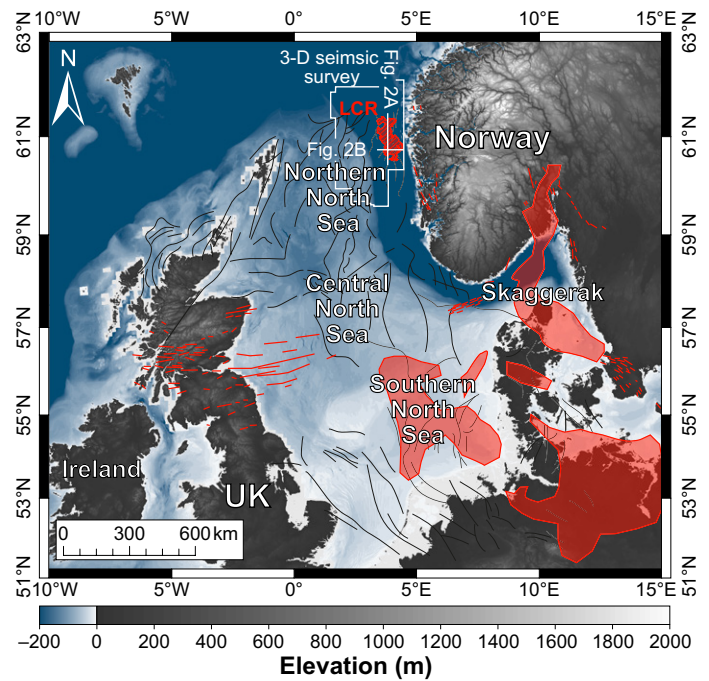
The LCR appears as a high-amplitude, positive-polarity seismic reflection in the lower crust at depths of 17.5–22 km depth (Figs. 2 and 3; Fig. DR1 in the Data Repository), and can be mapped continuously over ~2700 km² (Fig. 4; Fig. DR2). The LCR is ~97 km long (north-south) and ~62 km wide (east-west), consisting of several irregular “lobes” that laterally extend as much as ~20 km outwards from its center (Figs. 3B and 4; Animation DR1 in the Data Repository). These irregular lobes consist of several smaller,

*E-mail: thilo.wrona@uib.no

¹GSA Data Repository item 2019261, Text DR1 (seismic acquisition), Text DR2 (seismic processing), Text DR3 (lower crustal velocities), Text DR4 (tuning thickness), Figure DR1 (uninterpreted version of main Figure 2), Figure DR2 (uninterpreted and interpreted seismic section of main Figure 3E), and Animation DR1 (3-D animation of lower crustal intrusion), is available online at <http://www.geosociety.org/datarepository/2019/>, or on request from editing@geosociety.org.

CITATION: Wrona, T., et al., 2019, 3-D seismic images of an extensive igneous sill in the lower crust: *Geology*, v. 47, p. 729–733, <https://doi.org/10.1130/G46150.1>

Figure 1. Location map of North Sea showing area covered by three-dimensional (3-D) seismic survey (courtesy of CGG Worldwide, <https://www.cgg.com>) with lower-crustal reflection (LCR; white outline), magmatic dikes (red lines), tectonic faults (black lines), and volcanic rocks (red polygons) emplaced between late Carboniferous (ca. 300 Ma) and Late Triassic (ca. 220 Ma) as part of Skagerrak-centered large igneous province (Fossen and Dunlap, 1999; Bingen and Solli, 2009; Fazlikhani et al., 2017). Offshore, distribution of volcanic rocks is constrained by well and seismic data (Heeremans and Faleide, 2004; Torsvik et al., 2008; Phillips et al., 2017). Topography and bathymetry are from ESRI's World Elevation Service (Weatherall et al., 2015).



laterally connected “saucer” geometries (i.e., a flat inner surface that passes laterally into an inclined limb) (Figs. 3B and 4). These saucers are also the deepest parts of the LCR, extending down to a depth of 22 km, whereas the central part of the LCR is much shallower (17.5 km). The center of the LCR displays a series of elongated, 100–300-m-high vertical steps that cross-cut discontinuous, medium- to low-amplitude “background” reflections (Figs. 3A and 4). We observe several elongate high-amplitude anomalies aligned along these vertical steps in the horizontal plane (Figs. 3C and 4).

In general, the LCR shows: (1) high amplitudes, (2) a peak-trough wavelet, and (3) approximately equal peak and trough amplitudes, features that are typical of tuning effects (e.g., Widess, 1973; Robertson and Nogami,

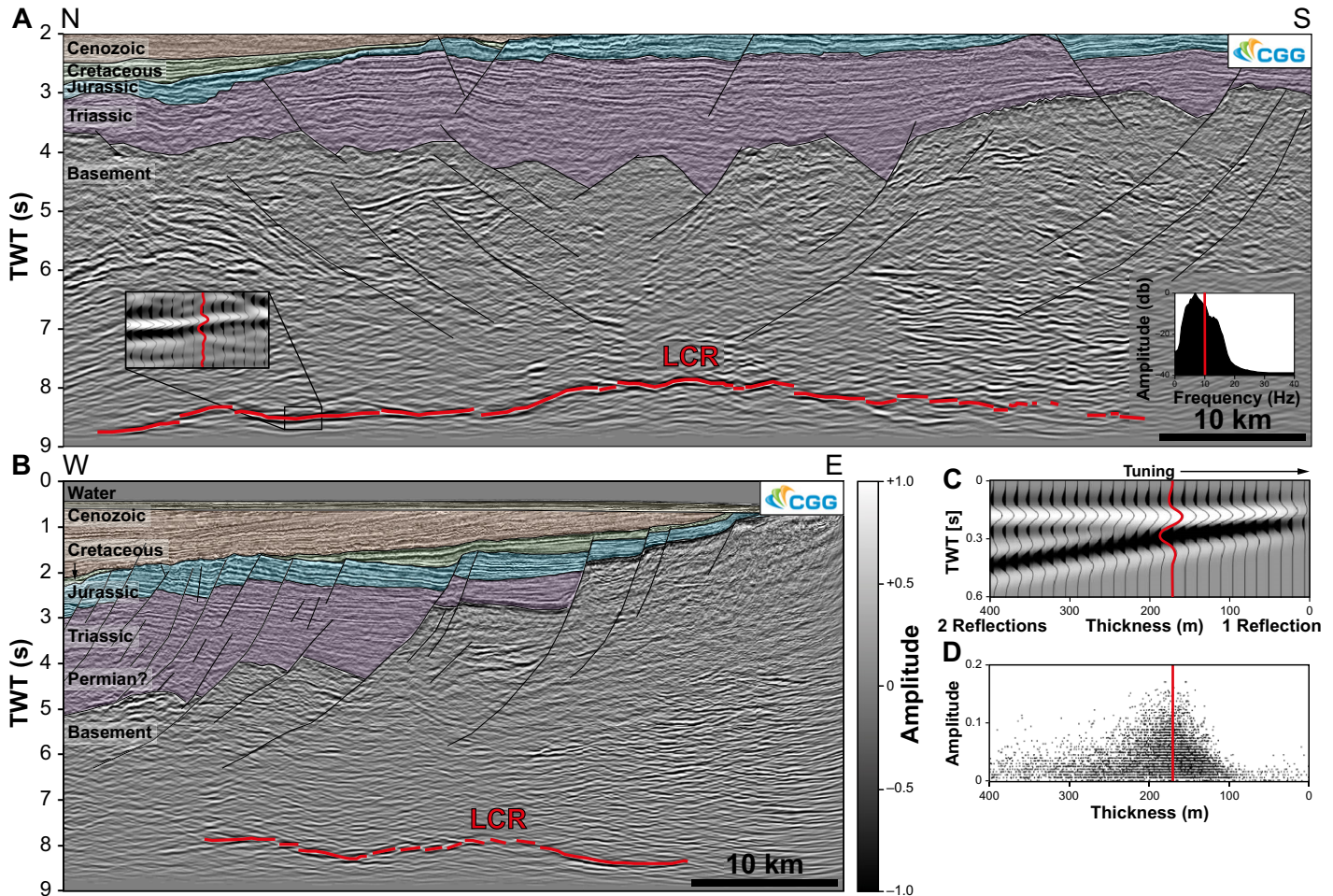


Figure 2. A: North-south seismic section showing lower-crustal reflection (LCR) in northern North Sea with closeup of seismic trace indicating peak-trough wavelet similar to tuning wedge (see C) and with frequency-amplitude spectrum showing dominant frequencies of 10 ± 2 Hz around LCR. See Figure 1 for seismic section location. B: East-west seismic section. See Figure 1 for location. C: Tuning wedge model based on acoustic impedance increase with depth. D: Thickness versus amplitude cross-plot of LCR with thicknesses calculated from time difference between top and bottom reflection using interval velocity of 7 km/s (Rosso, 2007). Note consistency of thickness estimates (180 ± 40 m) between C and D. Seismic data courtesy of CGG Worldwide (<https://www.cgg.com>). TWT—two-way travelttime.

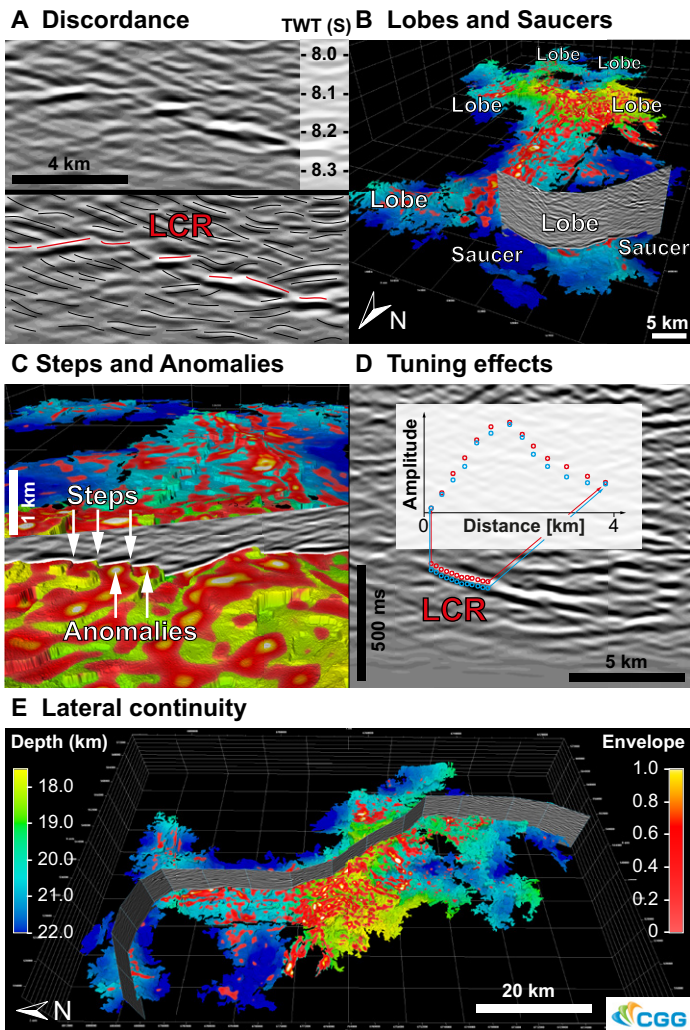


Figure 3. Seismic features of lower-crustal reflection (LCR) indicative of igneous intrusion in northern North Sea. **A:** Comparison between uninterpreted and interpreted seismic section showing discordance between LCR and host strata (cf. Cartwright and Hansen, 2006; Magee et al., 2016). **B:** “Lobe” geometries extending outwards from LCR (cf. Smallwood and Maresh, 2002; Magee et al., 2016) and “saucer” geometries showing flat inner sill that passes laterally into inclined limb (cf. Polteau et al., 2008; Haug et al., 2018; Infante-Paez and Marfurt, 2018; Schmiedel et al., 2019). **C:** Intrusive steps, i.e., laterally elongated vertical steps (cf. Hansen et al., 2004; Magee et al., 2016; McBride et al., 2018) with elongated amplitude anomalies (cf. Smallwood and Maresh, 2002). **D:** Tuning effects due to interference of waves originating from top and base of thin body. **E:** Lateral continuity of LCR over large area (~2700 km²) (cf. Magee et al., 2016) shown by three-dimensional surface and two-dimensional seismic section (see Fig. DR2 [see footnote 1]). Surfaces in B, C, and E show depth of LCR (in kilometers below sea-floor) overlain by amplitude envelope extracted along surface. Seismic data courtesy of CGG Worldwide (<https://www.cgg.com>).

1984; Sheriff and Geldart, 1995) (Figs. 2 and 3D). Tuning occurs when seismic waves originating from the top and base of a thin body interfere on their return to the surface (e.g., Brown, 2011). We can estimate the thickness of a body where constructive interference from top and base produces a single tuned response rather than two separate seismic reflections. Based on observed dominant frequencies of 10 ± 2 Hz (Fig. 2A) and seismic velocities of 6.9 ± 0.1 km/s for these basement rocks, derived from a recent wide-angle 2-D seismic survey (Rosso, 2007), we estimate that the LCR originates from a $\leq 180 \pm 40$ -m-thick body (Fig. 2C); this tuning thickness is consistent with an independent estimate based on an amplitude-versus-thickness cross-plot (Connolly, 2005; Francis, 2015) (Fig. 2D) (see Text DR4).

DISCUSSION

We observe that the LCR shows typical effects of tuning (e.g., equal peak and trough amplitudes; Fig. 3D), which implies that it originates from a thin layer rather than the top of a several-kilometers-thick rock volume (cf. Christiansson et al., 2000; Fichler et al., 2011). Furthermore, the suggested eclogitization (Christiansson et al., 2000) and serpentinization origins for the LCR (Fichler et al., 2011) are at odds with observed velocities and the polarity of the LCR. For example, while eclogitization was initially postulated based on inferred seismic velocities of >8 km/s in the region of the LCR (Christiansson et al., 2000), recent wide-angle 2-D reflection and refraction data reveal normal velocities of 6.9 ± 0.1 km/s (Rosso, 2007) (see Text DR3 for more details). In contrast, serpentinization reduces seismic velocities (Christensen, 2004), which would result in a downward decrease in acoustic impedance and a negative polarity reflection, rather than the normal polarity we observe for the LCR (e.g., Figs. 2 and 3).

After examining previous interpretations of the LCR, we now discuss other explanations for lower-crustal reflections. Reflections from highly strained rocks within a shear zone could explain the tuning effects, but shear zones are usually several kilometers thick in the lower crust and typically imaged as multiple, subparallel seismic reflections (Clerc et al., 2015; Fazlikhani et al., 2017). As such, it is difficult to explain the isolated, subhorizontal reflection we observe (e.g., Fig. 2) in terms of a ductile, lower-crustal shear zone.

Instead, we observe that the LCR shows the characteristic features of igneous intrusions observed in the field, seismic reflection data, and numerical models.

(1) The LCR cross-cuts numerous inclined, discontinuous “background” reflections that originate from the host stratigraphy (Fig. 3A). Discordance between igneous intrusions and the host stratigraphy is commonly observed in seismic images from sedimentary basins and develops when magma cross-cuts existing strata without offsetting it (e.g., Cartwright and Hansen, 2006; Magee et al., 2016; Eide et al., 2017).

(2) The LCR shows irregular lobes extending outward from its central axis (Fig. 3B). Similar lobes are commonly observed in igneous sills (i.e., tabular sheet intrusions) imaged by 3-D seismic reflection data, as well as those observed in field exposures, and form by incremental emplacement of discrete magma injections (e.g., Smallwood and Maresh, 2002; Schofield et al., 2012a; Magee et al., 2016).

(3) These lobes themselves comprise a series of saucers consisting of a flat inner surface that passes laterally into an inclined limb (Fig. 3B). Numerous sills observed in the field and in seismic reflection data and produced in numerical and analogue models display saucer-shaped morphologies, formed when a relatively flat sill develops transgressive inclined limbs in response to stress perturbations and/or host-rock deformation at its lateral tips (e.g., Malthe-Sørensen et al., 2004; Polteau et al., 2008; Haug et al., 2018; Schmiedel et al., 2019).

(4) The LCR contains several elongated, linear, vertical steps (Fig. 3C), which appear similar to intrusive steps formed during sheet propagation and are a record of magma flow (e.g., Hansen et al., 2004; Magee et al., 2016, 2018; McBride et al., 2018).

(5) The LCR displays laterally elongated amplitude anomalies (Fig. 3C), which likely relate to subtle, local variations in intrusion thickness and may correspond to magma flow channels (cf. Holness and Humphreys, 2003).

(6) The tuning effects displayed by the LCR are indicative of reflections emanating from a thin body (Figs. 2C and 3D), consistent with the seismic expression of relatively thin sills observed in real and synthetic seismic reflection data (<300 m; Magee et al., 2016).

(7) The LCR is continuous over a large area (~2700 km²) (Fig. 3E), a common feature of sills, which can extend over several hundreds of kilometers (e.g., Magee et al., 2016).

The combination of these observations supports our interpretation that the LCR originates from an igneous sill.

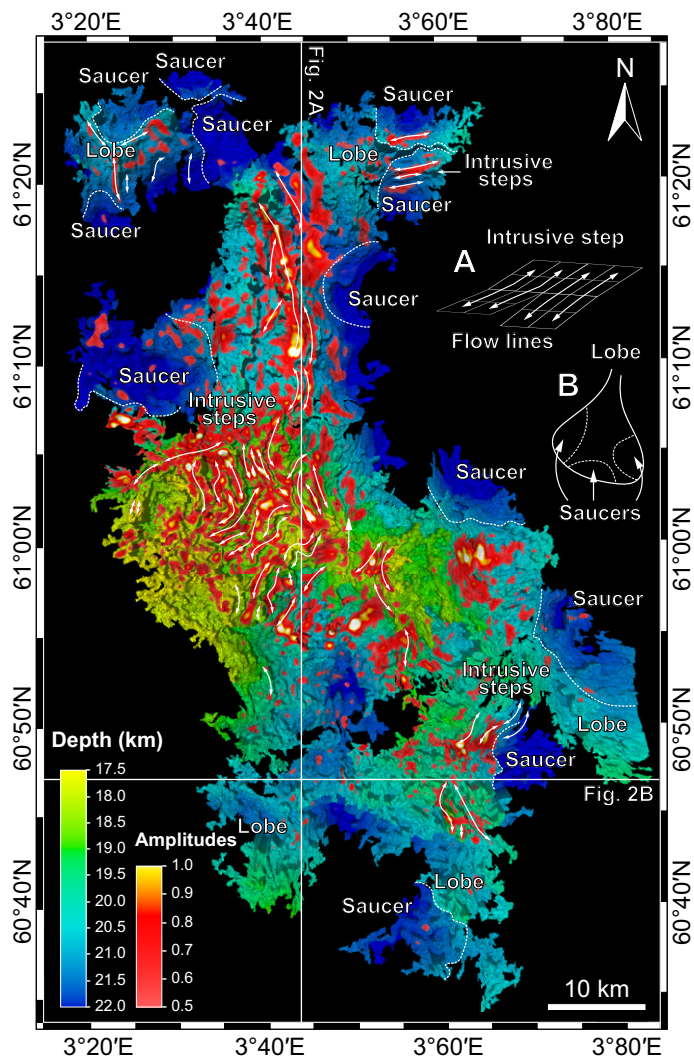


Figure 4. Three-dimensional (3-D) geometry of lower-crustal reflection (LCR) originating from igneous sill in northern North Sea. Evidence for LCR being igneous intrusion includes: (1) significant lateral continuity (~2700 km²) (cf. Magee et al., 2016); (2) irregular lobes extending outwards (cf. Smallwood and Maresh, 2002; Magee et al., 2016), (3) saucer-shaped geometries forming parts of these lobes (see B) (cf. Polteau et al., 2008; Haug et al., 2018; Infante-Paez and Marfurt, 2018; Schmiedel et al., 2019); (4) intrusive steps (cf. Hansen et al., 2004; Magee et al., 2016; McBride et al., 2018); and (5) elongated amplitude anomalies (cf. Smallwood and Maresh, 2002). Magma flow lines (white arrows) are drawn from elongated amplitude anomalies perpendicular to intrusive steps (see A). Depth conversion is based on shallow (0–5 km) checkshot and deep (5–22 km) seismic data (Rosso, 2007; Bell et al., 2014). 3-D animation of surface can be found in Data Repository (see footnote 1). Seismic data courtesy of CGG Worldwide (<https://www.cgg.com>).

IMPLICATIONS

We estimate a magma volume of 472 ± 161 km³ for the LCR by multiplying the surface area (~2700 km²) with the inferred tuning thickness (180 ± 40 m). While the LCR intrusion is less voluminous than the largest exposed or seismically imaged sills (e.g., sills in the Ferrar sill complex of Antarctica of up to 10^5 km³), it is still more extensive than most sills in the Karoo (South Africa) or Franklin (Canada) sill complexes (Cruden et al., 2017). The LCR intrusion volume is of the same order of magnitude as layered mafic intrusions emplaced in sedimentary rocks (see Cruden et al., 2017, their figure 1b) as well as stacked lower-crustal intrusions mapped in 2-D seismic reflection data from the North Atlantic margin (540–600 km³;

White et al., 2008). Constraining the composition of this intrusion is not possible given the uncertainty in measured velocity measurements (6.9 ± 0.1 km/s; Rosso, 2007) and the insensitivity of seismic velocities to compositional variations in igneous rocks (Behn and Kelemen, 2003; Bartzeko et al., 2005). In addition to our volume estimates, we constrain magma flow patterns within the LCR using intrusive steps (Fig. 3C) and amplitude anomalies (Figs. 3C and 4). Intrusive steps form because propagating sheets are commonly segmented, with individual segments intruding at slightly different structural levels (e.g., Schofield et al., 2012b; Magee et al., 2018). As magma intrusion continues and the segments inflate, they coalesce to form a throughgoing sill that contains vertical steps marking segment boundaries, with the long axes of steps and segments reflecting the initial sheet propagation direction (e.g., Schofield et al., 2012b; Magee et al., 2018). This process results in thickness variations, which translate into amplitude anomalies due to tuning effects (Magee et al., 2015). We observe these elongated amplitude anomalies on the LCR in map view (Fig. 4). The presence of steps and amplitude anomalies as long as 20 km, which may represent magma channels within the LCR, implies that emplacement occurred primarily through lateral flow, rather than by amalgamation of many small sills fed by dikes. While magma plumbing systems are typically depicted as dike dominated, with sills forming vertically stacked storage reservoirs in the lower or upper crust (e.g., Annen et al., 2005, 2015; Cashman et al., 2017; Edmonds et al., 2019), our observations highlight significant horizontal transport in the lower crust.

CONCLUSIONS

This study reveals a lower-crustal igneous intrusion in a continental rift (northern North Sea), which has long been considered magma poor. This sill is ~97 km long in the north-south and ~62 km wide in the east-west direction, showing evidence for significant lateral transport (as much as 20 km) of large volumes of magma (472 ± 161 km³). This study shows how advanced 3-D seismic imaging can help us understand magmatic processes occurring deep within the crust.

ACKNOWLEDGMENTS

We thank the journal editor (Mark Quigley) and three reviewers (Joe Cartwright, Lennon Infante-Paez, and Alexander Cruden) for their insightful reviews which led to a greatly improved manuscript. Financial support for this project was provided by the Norwegian Academy of Science and Letters (VISTA) and the University of Bergen. We thank CGG Worldwide (Paris, France), in particular Stein Åsheim, for the permission to use and publish these data. Furthermore, we thank Schlumberger for providing the software Petrel 2017 (<https://www.software.slb.com/products/petrel>), and Leo Zijerveld for information technology support.

REFERENCES CITED

- Abdelmalak, M.M., Faleide, J.I., Planke, S., Gernigon, L., Zastrozhnov, D., Shephard, G.E., and Myklebust, R., 2017, The *T*-reflection and the deep crustal structure of the Vøring Margin, offshore mid-Norway: *Tectonics*, v. 36, p. 2497–2523, <https://doi.org/10.1002/2017TC004617>.
- Annen, C., Blundy, J.D., and Sparks, R.S.J., 2005, The genesis of intermediate and silicic magmas in deep crustal hot zones: *Journal of Petrology*, v. 47, p. 505–539, <https://doi.org/10.1093/petrology/egi084>.
- Annen, C., Blundy, J.D., Leuthold, J., and Sparks, R.S.J., 2015, Construction and evolution of igneous bodies: Towards an integrated perspective of crustal magmatism: *Lithos*, v. 230, p. 206–221, <https://doi.org/10.1016/j.lithos.2015.05.008>.
- Austrheim, H., 1987, Eclogitization of lower crustal granulites by fluid migration through shear zones: *Earth and Planetary Science Letters*, v. 81, p. 221–232, [https://doi.org/10.1016/0012-821X\(87\)90158-0](https://doi.org/10.1016/0012-821X(87)90158-0).
- Bartzeko, A., Delius, H., and Pechinig, R., 2005, Effect of compositional and structural variations on log responses of igneous and metamorphic rocks. I: Mafic rocks, in Harvey, P.K., et al., eds., *Petrophysical Properties of Crystalline Rocks*: Geological Society of London Special Publication 240, p. 255–278, <https://doi.org/10.1144/GSL.SP.2005.240.01.19>.
- Behn, M.D., and Kelemen, P.B., 2003, Relationship between seismic P-wave velocity and the composition of anhydrous igneous and meta-igneous rocks: *Geochemistry Geophysics Geosystems*, v. 4, 1041, <https://doi.org/10.1029/2002GC000393>.
- Bell, R.E., Jackson, C.A.-L., Whipp, P.S., and Clements, B., 2014, Strain migration during multiphase extension: Observations from the northern North Sea: *Tectonics*, v. 33, p. 1936–1963, <https://doi.org/10.1002/2014TC003551>.

- Bingen, B., and Solli, A., 2009, Geochronology of magmatism in the Caledonian and Sveconorwegian belts of Baltica: Synopsis for detrital zircon provenance studies: *Norsk Geologisk Tidsskrift*, v. 89, p. 267–290.
- Bingen, B., Nordgulen, Ø., and Viola, G., 2008, A four-phase model for the Sveconorwegian orogeny, SW Scandinavia: *Norsk Geologisk Tidsskrift*, v. 88, p. 43–72.
- Brown, A.R., 2011, Interpretation of Three-Dimensional Seismic Data (seventh edition): American Association of Petroleum Geologists Memoir 42 and Society of Exploration Geophysicists Investigations in Geophysics 9, 665 p., <https://doi.org/10.1190/1.9781560802884>.
- Cartwright, J., and Hansen, D.M., 2006, Magma transport through the crust via interconnected sill complexes: *Geology*, v. 34, p. 929–932, <https://doi.org/10.1130/G22758A.1>.
- Cashman, K.V., Sparks, R.S.J., and Blundy, J.D., 2017, Vertically extensive and unstable magmatic systems: A unified view of igneous processes: *Science*, v. 355, eaag3055, <https://doi.org/10.1126/science.aag3055>.
- Christensen, N.I., 2004, Serpentinities, peridotites, and seismology: *International Geology Review*, v. 46, p. 795–816, <https://doi.org/10.2747/0020-6814.46.9.795>.
- Christiansson, P., Faleide, J.I., and Berge, A.M., 2000, Crustal structure in the northern North Sea: An integrated geophysical study, in Nøttvedt, A., ed., Dynamics of the Norwegian Margin: Geological Society of London Special Publication 167, p. 15–40, <https://doi.org/10.1144/GSL.SP.2000.167.01.02>.
- Clerc, C., Jolivet, L., and Ringenbach, J.-C., 2015, Ductile extensional shear zones in the lower crust of a passive margin: *Earth and Planetary Science Letters*, v. 431, p. 1–7, <https://doi.org/10.1016/j.epsl.2015.08.038>.
- Connolly, P., 2005, Net pay estimation from seismic attributes: Paper F016 presented at the European Association of Geoscientists and Engineers 67th Conference and Exhibition, Madrid, Spain, 13–16 June.
- Cruden, A.R., McCaffrey, K.J.W., and Bungler, A.P., 2017, Geometric scaling of tabular igneous intrusions: Implications for emplacement and growth, in Breiterkreuz, C., and Rocchi, S., eds., Physical Geology of Shallow Magmatic Systems: Dykes, Sills and Laccoliths: Springer, p. 11–38, https://doi.org/10.1007/11157_2017_1000.
- Edmonds, M., Cashman, K.V., Holness, M., and Jackson, M., 2019, Architecture and dynamics of magma reservoirs: *Philosophical Transactions of the Royal Society of London A: Mathematical, Physical and Engineering Sciences*, v. 377, 20180298, <https://doi.org/10.1098/rsta.2018.0298>.
- Eide, C.H., Schofield, N., Lecomte, I., Buckley, S.J., and Howell, J.A., 2017, Seismic interpretation of sill complexes in sedimentary basins: Implications for the sub-sill imaging problem: *Journal of the Geological Society*, v. 175, p. 2017–2096, <https://doi.org/10.1144/jgs2017-096>.
- Fazlkhani, H., Fossen, H., Gawthorpe, R.L., Faleide, J.I., and Bell, R.E., 2017, Basement structure and its influence on the structural configuration of the northern North Sea rift: *Tectonics*, v. 36, p. 1151–1177, <https://doi.org/10.1002/2017TC004514>.
- Fichler, C., Odinsen, T., Rueslåtten, H., Olesen, O., Vindstad, J.E., and Wienecke, S., 2011, Crustal inhomogeneities in the Northern North Sea from potential field modeling: Inherited structure and serpentinites?: *Tectonophysics*, v. 510, p. 172–185, <https://doi.org/10.1016/j.tecto.2011.06.026>.
- Fossen, H., and Dunlap, W.J., 1999, On the age and tectonic significance of Permo-Triassic dikes in the Bergen-Sunnhordland region, southwestern Norway: *Norsk Geologisk Tidsskrift*, v. 79, p. 169–178, <https://doi.org/10.1080/002919699433807>.
- Francis, A., 2015, A simple guide to seismic amplitudes and detuning: *GEOExPro*, v. 12, no. 5, p. 68–72.
- Hansen, D.M., Cartwright, J.A., and Thomas, D., 2004, 3D seismic analysis of the geometry of igneous sills and sill junction relationships, in Davies, R.J., et al., eds., 3D Seismic Technology: Application to the Exploration of Sedimentary Basins: Geological Society of London Memoir 29, p. 199–208, <https://doi.org/10.1144/GSL.MEM.2004.029.01.19>.
- Haug, Ø.T., Galland, O., Souloumiac, P., Souche, A., Guldstrand, F., Schmiedel, T., and Maillot, B., 2018, Shear versus tensile failure mechanisms induced by sill intrusions: Implications for emplacement of conical and saucer-shaped intrusions: *Journal of Geophysical Research: Solid Earth*, v. 123, p. 3430–3449, <https://doi.org/10.1002/2017JB015196>.
- Heeremans, M., and Faleide, J.I., 2004, Late Carboniferous–Permian tectonics and magmatic activity in the Skagerrak, Kattegat and the North Sea, in Wilson, M., et al., eds., Permo-Carboniferous Magmatism and Rifting in Europe: Geological Society of London Special Publication 223, p. 157–176, <https://doi.org/10.1144/GSL.SP.2004.223.01.07>.
- Holness, M.B., and Humphreys, M.C.S., 2003, The Traigh Bhàn na Sgùrra sill, Isle of Mull: Flow localization in a major magma conduit: *Journal of Petrology*, v. 44, p. 1961–1976, <https://doi.org/10.1093/petrology/egg066>.
- Huisman, R., and Beaumont, C., 2011, Depth-dependent extension, two-stage breakup and cratonic underplating at rifted margins: *Nature*, v. 473, p. 74–78, <https://doi.org/10.1038/nature09988>.
- Infante-Paez, L., and Marfurt, K.J., 2018, In-context interpretation: Avoiding pitfalls in misidentification of igneous bodies in seismic data: *Interpretation*, v. 6, p. SL29–SL42, <https://doi.org/10.1190/Int-2018-0076.1>.
- Magee, C., Maharaj, S.M., Wrona, T., and Jackson, C.A.-L., 2015, Controls on the expression of igneous intrusions in seismic reflection data: *Geosphere*, v. 11, p. 1024–1041, <https://doi.org/10.1130/GES01150.1>.
- Magee, C., et al., 2016, Lateral magma flow in mafic sill complexes: *Geosphere*, v. 12, p. 809–841, <https://doi.org/10.1130/GES01256.1>.
- Magee, C., Muirhead, J., Schofield, N., Walker, R.J., Galland, O., Holford, S., Spacapan, J., Jackson, C.A.-L., and McCarthy, W., 2018, Structural signatures of igneous sheet intrusion propagation: *Journal of Structural Geology*, <https://doi.org/10.1016/j.jsg.2018.07.010>.
- Malthe-Sørensen, A., Planke, S., Svensen, H., and Jamtveit, B., 2004, Formation of saucer-shaped sills: Physical geology of high-level magmatic systems, in Breiterkreuz, C., and Petford, N., eds., Physical Geology of High-Level Magmatic Systems: Geological Society of London Special Publication 234, p. 215–227, <https://doi.org/10.1144/GSL.SP.2004.234.01.13>.
- Maystrenko, Y.P., Olesen, O., Ebbing, J., and Nasuti, A., 2017, Deep structure of the northern North Sea and southwestern Norway based on 3D density and magnetic modelling: *Norsk Geologisk Tidsskrift*, v. 97, p. 169–210, <https://doi.org/10.17850/njg97-3-01>.
- McBride, J.H., Keach, R.W., Lectaru, H.E., and Smith, K.M., 2018, Visualizing Precambrian basement tectonics beneath a carbon capture and storage site: Illinois Basin: *Interpretation*, v. 6, p. T257–T270, <https://doi.org/10.1190/Int-2017-0116.1>.
- Phillips, T.B., Magee, C., Jackson, C.A.-L., and Bell, R.E., 2017, Determining the three-dimensional geometry of a dike swarm and its impact on later rift geometry using seismic reflection data: *Geology*, v. 46, p. 119–122, <https://doi.org/10.1130/G39672.1>.
- Planke, S., Rasmussen, T., Rey, S.S., and Myklebust, R., 2005, Seismic characteristics and distribution of volcanic intrusions and hydrothermal vent complexes in the Vøring and Møre basins, in Doré, A.G., and Vining, B.A., eds., Petroleum Geology: North-West Europe and Global Perspectives—Proceedings of the 6th Petroleum Geology Conference: Geological Society of London Petroleum Geology Conference Series 6, p. 833–844, <https://doi.org/10.1144/0060833>.
- Polteau, S., Mazzini, A., Galland, O., Planke, S., and Malthe-Sørensen, A., 2008, Saucer-shaped intrusions: Occurrences, emplacement and implications: *Earth and Planetary Science Letters*, v. 266, p. 195–204, <https://doi.org/10.1016/j.epsl.2007.11.015>.
- Robertson, J.D., and Nogami, H.H., 1984, Complex seismic trace analysis of thin beds: *Geophysics*, v. 49, p. 344–352, <https://doi.org/10.1190/1.1441670>.
- Rosso, A.E., 2007, Deep crustal geometry: An integrated geophysical study of an exhumed eclogite terrain, Bergen area, southwest Norway [M.S. thesis]: Laramie, University of Wyoming, 133 p.
- Schmiedel, T., Galland, O., Haug, Ø.T., Dumazer, G., and Breiterkreuz, C., 2019, Coulomb failure of Earth's brittle crust controls growth, emplacement and shapes of igneous sills, saucer-shaped sills and laccoliths: *Earth and Planetary Science Letters*, v. 510, p. 161–172, <https://doi.org/10.1016/j.epsl.2019.01.011>.
- Schofield, N., Heaton, L., Holford, S.P., Archer, S.G., Jackson, C.A.-L., and Jolley, D.W., 2012a, Seismic imaging of 'broken bridges': Linking seismic to outcrop-scale investigations of intrusive magma lobes: *Journal of the Geological Society*, v. 169, p. 421–426, <https://doi.org/10.1144/0016-76492011-150>.
- Schofield, N.J., Brown, D.J., Magee, C., and Stevenson, C.T., 2012b, Sill morphology and comparison of brittle and non-brittle emplacement mechanisms: *Journal of the Geological Society*, v. 169, p. 127–141, <https://doi.org/10.1144/0016-76492011-078>.
- Sheriff, R.E., and Geldart, L.P., 1995, *Exploration Seismology* (second edition): Cambridge, UK, Cambridge University Press, <https://doi.org/10.1017/CBO9781139168359>.
- Smallwood, J.R., and Maresh, J., 2002, The properties, morphology and distribution of igneous sills: Modelling, borehole data and 3D seismic from the Faroe-Shetland area, in Jolley, D.W., and Bell, B.R., eds., The North Atlantic Igneous Province: Stratigraphy, Tectonic, Volcanic and Magmatic Processes: Geological Society of London Special Publication 197, p. 271–306, <https://doi.org/10.1144/GSL.SP.2002.197.01.11>.
- Torsvik, T.H., Smethurst, M.A., Burke, K., and Steinberger, B., 2008, Long term stability in deep mantle structure: Evidence from the ~300 Ma Skagerrak-Centered Large Igneous Province (the SCLIP): *Earth and Planetary Science Letters*, v. 267, p. 444–452, <https://doi.org/10.1016/j.epsl.2007.12.004>.
- Trude, J., Cartwright, J., Davies, R.J., and Smallwood, J., 2003, New technique for dating igneous sills: *Geology*, v. 31, p. 813–816, <https://doi.org/10.1130/G19559.1>.
- Weatherall, P., Marks, K.M., Jakobsson, M., Schmitt, T., Tani, S., Arndt, J.E., Rovere, M., Chayes, D., Ferrini, V., and Wigley, R., 2015, A new digital bathymetric model of the world's oceans: *Earth and Space Science*, v. 2, p. 331–345, <https://doi.org/10.1002/2015EA000107>.
- White, R.S., et al., 2008, Lower-crustal intrusion on the North Atlantic continental margin: *Nature*, v. 452, p. 460–464, <https://doi.org/10.1038/nature06687>.
- Widess, M.B., 1973, How thin is a thin bed?: *Geophysics*, v. 38, p. 1176–1180, <https://doi.org/10.1190/1.1440403>.

Printed in USA